

## Fabrication and electrochemical performance of solid oxide fuel cell components by atmospheric and suspension plasma spray

XIA Wei-sheng(夏卫生)<sup>1,2</sup>, YANG Yun-zhen(杨云珍)<sup>3</sup>, ZHANG Hai-ou(张海鸥)<sup>2</sup>, WANG Gui-lan(王桂兰)<sup>1</sup>

1. State Key Laboratory of Materials Processing and Die & Mould Technology,  
Huazhong University of Science and Technology, Wuhan 430074, China;

2. State Key Laboratory of Digital Manufacturing Equipment and Technology,  
Huazhong University of Science and Technology, Wuhan 430074, China;

3. College of Automotive Engineering, Wuhan University of Technology, Wuhan 430070, China

Received 10 August 2009; accepted 15 September 2009

**Abstract:** The theory of functionally graded material (FGM) was applied in the fabrication process of PEN (Positive-Electrolyte-Negative), the core component of solid oxide fuel cell (SOFC). To enhance its electrochemical performance, the functionally graded PEN of planar SOFC was prepared by atmospheric plasma spray (APS). The cross-sectional SEM micrograph and element energy spectrum of the resultant PEN were analyzed. Its interface resistance was also compared with that without the graded layers to investigate the electrochemical performance enhanced by the functionally graded layers. Moreover, a new process, suspension plasma spray (SPS) was applied to preparing the SOFC electrolyte. Higher densification of the coating by SPS, 1.61%, is observed, which is helpful to effectively improve its electrical conductivity. The grain size of the electrolyte coating fabricated by SPS is also smaller than that by APS, which is more favourable to obtain the dense electrolyte coatings. To sum up, all mentioned above can prove that the hybrid process of APS and SPS could be a better approach to fabricate the PEN of SOFC stacks, in which APS is for porous electrodes and SPS for dense electrolyte.

**Key words:** solid oxide fuel cell; atmospheric plasma spray; suspension plasma spray; functionally graded material; fabricating process; electrochemical performance

### 1 Introduction

Solid oxide fuel cell (SOFC) has drawn keen attention because of its high energy conversion efficiency (about 65%[1]), low environmental hazards, high power density and other merits. As a promising energy conversion device in the 21st century, SOFC is expected to realize commercialization within a few years[2–4]. However, fabricating high performance PEN (Positive-Electrolyte-Negative), the core component of SOFC, is still expensive and time-consuming up to now. Hence, it is necessary and essential to improve the current technologies or to introduce new fabrication approaches.

Atmospheric plasma spray (APS) is a promising candidate for the porous SOFC electrodes due to its processing characteristics, and is suitable to rapidly

deposit coatings for almost all kinds of materials[5]. Due to its flexibility and low cost, much research efforts have been devoted to prepare electrolyte[6], porous anode[7], cathode[8] and even the whole PEN[4] of SOFCs. However, it is difficult or impossible to prepare the full density electrolyte layer by APS due to its inherent lamellar microstructure. Yttria stabilized zirconia (YSZ) is a most popular material for SOFC electrolyte. But the thickness of YSZ coatings sprayed by APS is always in 100  $\mu\text{m}$ –1 mm with the porosity of 1%–20%[9]. To improve the performance of the SOFC stack, the electrolyte thickness should be kept typically in 15–30  $\mu\text{m}$ . The thin electrolyte can decrease the operating temperature of SOFCs in order to extend their life-time depending on the mechanical and chemical stabilities of materials and to reduce production costs.

To overcome these restrictions, suspension plasma spray (SPS), a new improved technology, has been

**Foundation item:** Project(50675081) supported by the National Natural Science Foundation of China; Project(20080440940) supported by China Postdoctoral Science Foundation

**Corresponding author:** XIA Wei-sheng; Tel: +86-27-87557394; E-mail: [xiatianhust@hotmail.com](mailto:xiatianhust@hotmail.com)

DOI: 10.1016/S1003-6326(09)60066-2

developed to spray finely structured coatings by injecting a suspension containing nano- or micro-sized particles [9–12]. It is attractive for various high performance applications.

In this work, the theory of functionally graded material (FGM) was applied in the fabrication process to enhance electrochemical performance of SOFC. The functionally graded PEN of planar SOFC was prepared by APS, and the cross-sectional SEM micrograph and element energy spectrum of the resultant PEN were analyzed. Its interface resistance was also compared with that without the graded layers to investigate the electrochemical performance enhanced by the functionally graded layers. Moreover, SPS was applied to fabricating the dense electrolyte, and its new process characteristics were introduced via the comparison with APS.

## 2 Experimental

### 2.1 Spray materials and suspensions

Commercial 8YSZ powder (EE-Tec. Inc., Shanghai, China) was selected to prepare the electrolyte coating, as shown in Fig.1. It has a uniform distribution of particle size, and the specific surface area is  $16 \text{ m}^2/\text{g}$ . 8YSZ and Ni (45%, volume fraction) powders were mixed for the starting anode material. In order to increase the porosity of the SOFC anode, a quantity of carbon powder was added to the anode material. For good flowability in the APS process, the particle size distribution was adjusted in the range of 90–120  $\mu\text{m}$ .

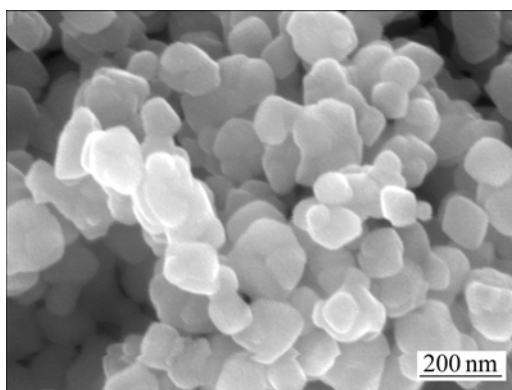


**Fig.1** SEM micrograph of YSZ powder

Considering the good chemical-thermal stability and high electric conductivity, Perovskite-type  $\text{La}_{0.8}\text{Sr}_{0.2}\text{Co}_{0.5}\text{Fe}_{0.5}\text{O}_3$  (LSCF) primary powder was prepared via the sol-gel route for the cathode powder[13]. The SEM image of the primary powder is shown in Fig.2. The granularity distribution of LSCF powder is uniform and in the range of 600 nm–1.5  $\mu\text{m}$ . For the APS application, the particle size distribution was adjusted in the range of

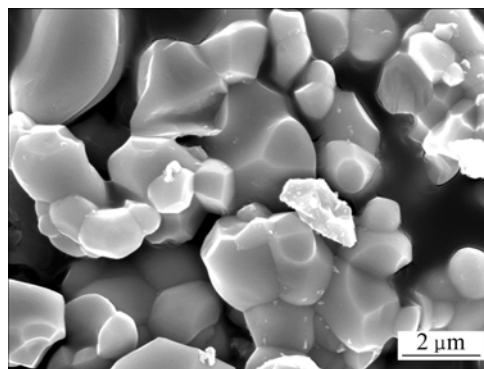


**Fig.2** SEM micrograph of LSCF powder

90–120  $\mu\text{m}$ .

The YSZ suspension was prepared and injected in the plasma jet. This suspension mainly consisted of ethanol with a powder mass percentage of 8% and polyvinyl alcohol as the dispersant.

### 2.2 Spray processes

APS was performed with the plasma-spray equipment typed GP-80, and an 8 mm internal diameter anode nozzle was selected. The FTI-1 volumetric powder feeding device self-designed was applied in the spraying of the functionally graded PENs. In particular, a Motoman-UP20 robot (Shougang Motoman Robot Corp., Beijing, China) was used, which was convenient for the adjustment and control of process parameters.

According to the FGM theory, if the graded layers consist of the materials of electrodes and electrolyte, their properties can be transmitted from electrodes to electrolyte and the mismatches between electrodes and electrolyte can also be improved as well as their electrochemical performance. In this work, two types of PEN are prepared for the comparison: one only contains cathode and electrolyte (in Fig.3(a)); the other consists of cathode, cathode graded layer and electrolyte (in Fig.3(b)). Spray parameters are listed in Table 1.

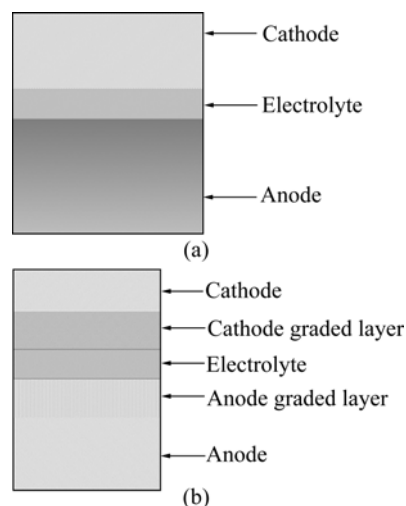


**Fig.3** PEN structures without (a) and with (b) two graded layers

Schematic diagram of the experimental system for SPS is indicated in Fig.4(a). The liquid feedstock system is composed of three stainless steel tanks, in which suspension is stored, stirred and mixed continually by the propeller fixed in the bottom of the tank. These three tanks can provide one or three different suspensions/solutions to fabricate a whole PEN or the composite anode/cathode in interval or continuous mode. During the SPS process, tanks are pressured with compressed air ( $N_2$ ) monitored and controlled with a rotor flow meter and a pressure regulating valve. It is worth noting that the momentum of liquid droplets has to be high enough to ensure their penetration into the core of plasma jet. Hence, the atomized nozzle was self-designed with three inlets for suspensions and one for the atomizing gas. Picture of the suspension injection and drops is shown in Fig.4(b). The feeding pressure of the tank and the suspension inlets can be varied to modify the drop velocities. The spray parameters during the SPS process are listed in Table 2.

### 2.3 Characterization

The phase structure and grain size of powders and coatings were identified by X-ray diffractometer (X' Pert Pro, Phillips Co. Holand) with  $Cu K_{\alpha}$  radiation (40 kV,

40 mA). Scans were performed from  $20^{\circ}$  to  $90^{\circ}$  ( $2\theta$ ) with a step size of  $0.017^{\circ}$ . The cross-sectional morphology of sprayed coatings was investigated by field emission scanning electron microscope (FESEM, FEI-Sirion 200, Phillips Co. Holand).

Electrochemical testing was carried out to measure the resistances of the two kinds of PENs in this work. The AC impedance device (VMP/2, Princeton Applied Research Corp., USA) was applied to detecting their electrical conductivity with a two-electrode configuration. Tests were performed under the air and nitrogen conditions from 500 to 800  $^{\circ}C$ . Impedance measurements were carried out at open circuit voltage (OCV) with the AC voltage amplitude of 10 mV over a frequency range of 0.01 Hz–200 kHz, depending on the measurement temperature.

## 3 Results and discussion

### 3.1 XRD characterization

XRD patterns of YSZ powder and sprayed coatings by APS and SPS are shown in Fig.5. The diffraction analysis reveals that all of the peaks are associated with prime YSZ powder. There are no variation of the

**Table 1** Processing parameters of PEN fabricated by APS

Material	Plasma power/kW	Powder feeding rate/(g·min <sup>-1</sup> )	Scanning velocity/(mm·s <sup>-1</sup> )	Scanning step/mm	Spray angle/( $^{\circ}$ )	Spraying time/min
Ni+YSZ	28	60	300	12	65	30
Anode graded layer	36	25	300	11/10	75–82	21
YSZ	39	30	300	10	90	21
Cathode graded layer	36	25	300	10/11	82–75	21
LSCF	32	50	300	10	65	25

**Table 2** Suspension plasma spray parameters

Current/A	Voltage/V	Plasma gas flow rate/(L·min <sup>-1</sup> )		Flow rate of powder carrier gas/(L·min <sup>-1</sup> )	Spray distance/mm
		Ar	$N_2$		
600	50	25	10	3.5	60

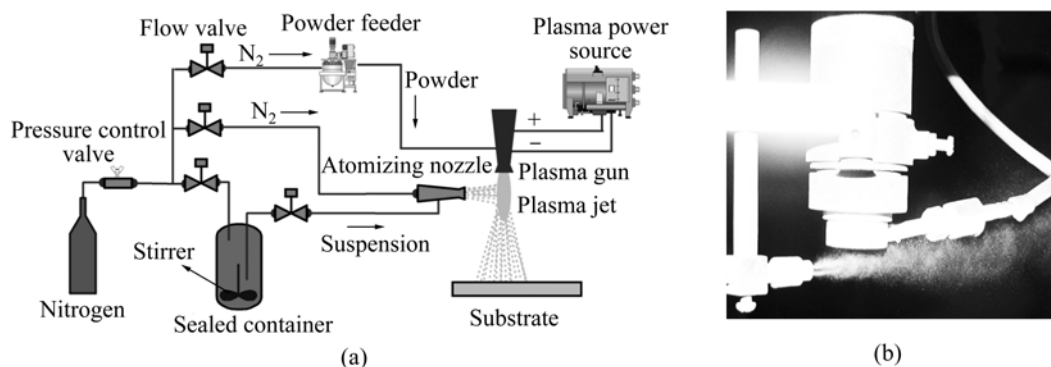


**Fig.4** Experimental set-up of SPS and APS (a) and picture of suspension injection and drops (b)

diffraction peak position in the X-ray diffraction patterns. This indicates that the main phase and chemical compositions are unchanged, and only cubic phase is detected in YSZ powder and coatings sprayed by APS or SPS. The powder peak is wider than as-sprayed coatings owing to its fine grain size, and no undesirable second phase is observed. The average grain size of YSZ powder calculated by Scherrer formula is 37.1 nm. Peak widths of as-sprayed coatings are narrow, which indicates that the grains grow up during both the two spray processes. The grain size of YSZ coatings fabricated by APS is 57.3 nm, while that is only 42 nm by SPS. Therefore, SPS has the potential of refining grain, which is beneficial for the fine and dense coatings.

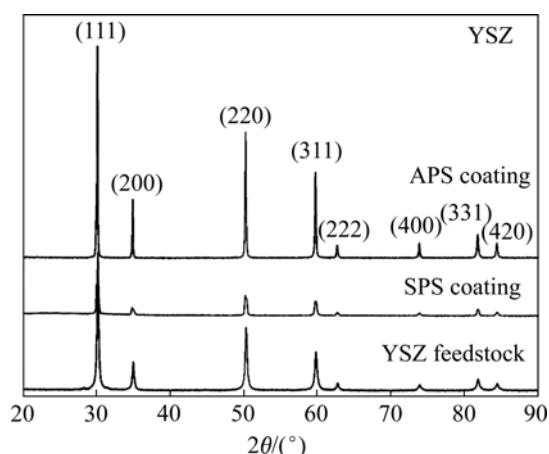


**Fig.5** XRD patterns of YSZ powder and sprayed coatings by APS and SPS

Fig.6 shows XRD patterns of LSCF powder and sprayed coating by APS. The peaks of LSCF powder are thin and narrow, which indicates the grain is fine. Diffraction peaks for rhombohedral perovskite structure are observed and the pure perovskite-type LSCF is synthesized with no desirable second phase. The grain

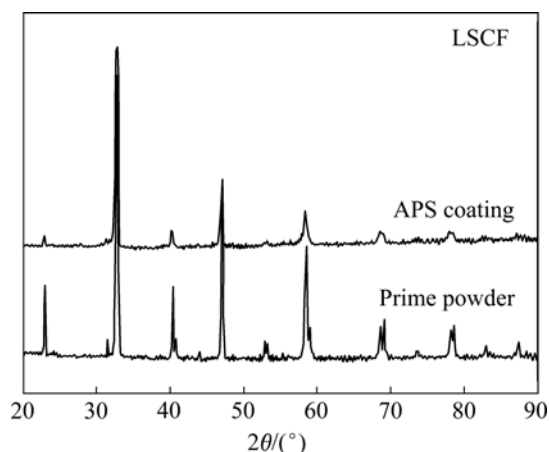


**Fig.6** XRD patterns of LSCF powder and sprayed coating by APS

size of  $\text{La}_{0.8}\text{Sr}_{0.2}\text{Co}_{0.5}\text{Fe}_{0.5}\text{O}_3$  powder determined by Scherrer formula is 860 nm and there is no phase transition during the APS process. Hence, this powder can meet the requirements of SOFC cathode layer prepared by APS.

### 3.2 Functionally graded PEN fabricated by APS

The cross-sectional SEM micrograph of planar PEN is shown in Fig.7(a). The PEN is composed of anode, anode graded layer, electrolyte, cathode graded layer and cathode. The thicknesses of the anode, the electrolyte and the cathode are 60, 30, and 40  $\mu\text{m}$ , respectively. In order to avoid the increase of the cell resistance, the graded layer only has the thickness of 25–30  $\mu\text{m}$ . In the two graded layers between the corresponding electrodes and the electrolyte, the material compositions gradually vary and component layers contact tightly. The porosity of the anode graded layer changes gradually from high to low, whereas that of the cathode graded layer gradually changes from low to high.

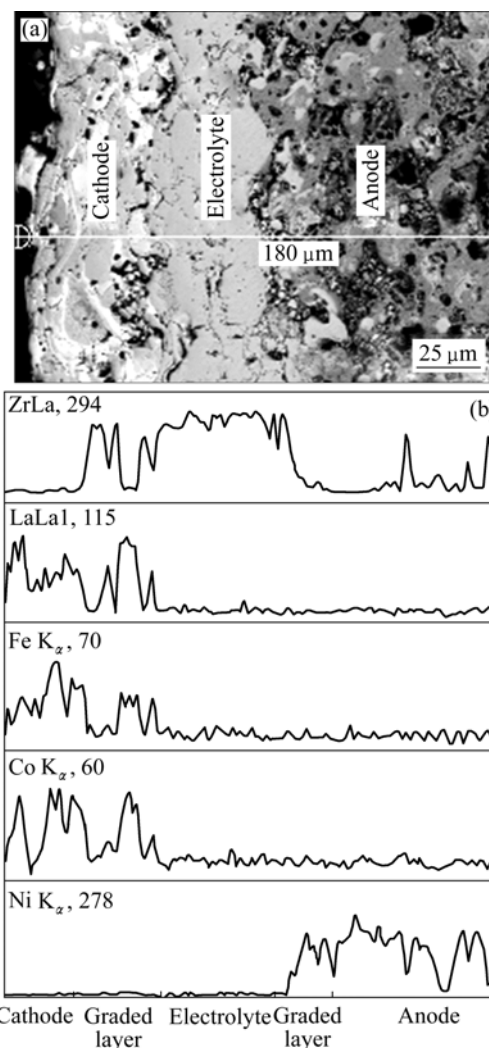


**Fig.7** Cross-sectional SEM photograph (a) and element energy spectrum (b) of planar PEN with graded layers

According to the energy spectral analysis shown in Fig.7(b), four elements (La, Sr, Fe, Co) are observed in the cathode layer, two (Y, Zr) are in the electrolyte and three (Y, Zr, Ni) are in the anode. Moreover, the material compositions in anode and cathode graded layers gradually change. Based on the FGM theory, the performances of the graded layers gradually vary due to their varying material elements. Therefore, not only the bonding states between the different components of the SOFC are improved, but also the mismatch of their thermal expansion coefficients is released.

The Arrhenius curves ( $\ln\sigma - 1/T$ ) of the electrical conductivity and temperature are presented in Fig.8. It can be observed that the logarithmic conductivities ( $\ln\sigma$ ) of the two PENs vary linearly with the  $1/T$  in the tested temperature range. The grain resistance and the interface contact resistance both decrease with the increase of test temperature. The interface resistance of the resultant PEN with the graded layers (Fig.8(b)) is far less than that without the graded layers (Fig.8(a)). However, due to the obvious variation of the material compositions and microstructure, the interface resistance of the PEN without the graded layer increases sharply. Hence, the FGM PEN with graded layers shows much better electrochemical performance than that without graded layers, especially at low temperature.

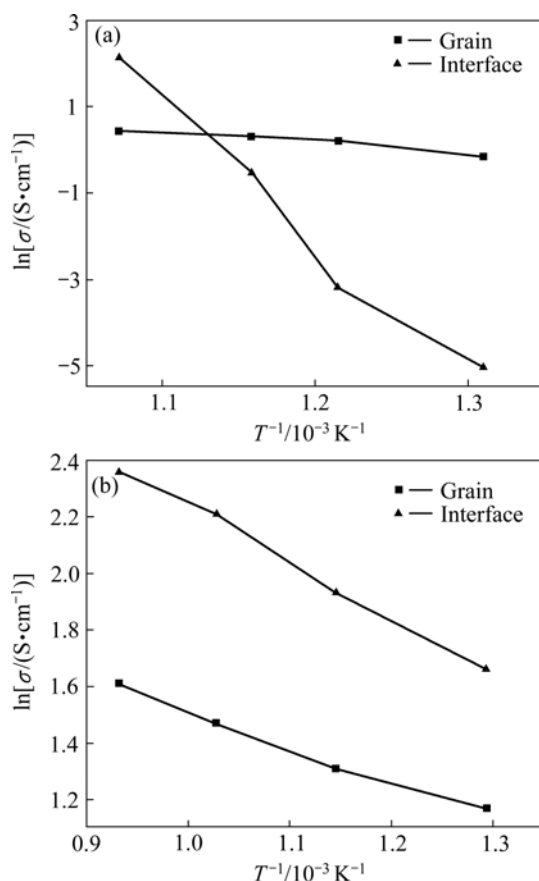


**Fig.8** Electrical conductivity curves of PENs without (a) and with (b) graded layers

### 3.3 Dense electrolyte sprayed by SPS

SEM photograph of the electrolyte coating by SPS is illustrated in Fig.9. The porosity of the electrolyte coating is 1.61% determined by the metallographic image method with the thickness of 160  $\mu m$ , and no connected pores are observed through its thickness direction. These cases can meet the dense and gas tightness requirements of electrolyte during the SOFC operating process. The local dense area in the electrolyte coating is shown in Fig.9(b).

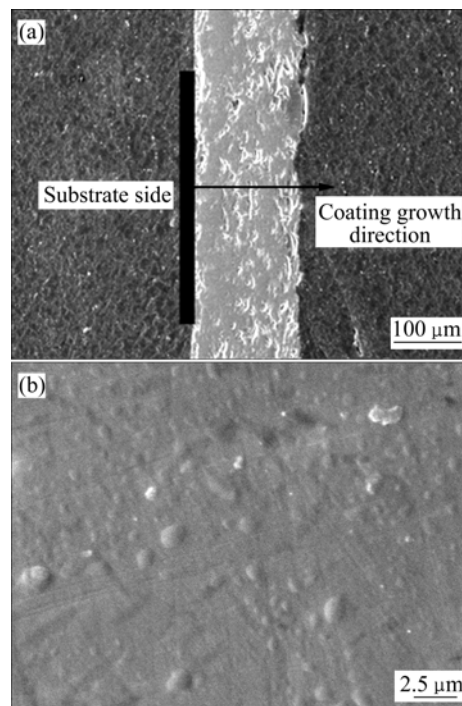


**Fig.9** SEM micrographs of cross-section for electrolyte fabricated by SPS: (a) General view; (b) Local dense area

### 3.4 Discussion

Cross-sectional SEM micrographs of electrolyte coatings by APS are shown in Fig. 10. The forming drawbacks, voids and cracks are observed. APS can also achieve higher density, which is associated with material nature, in-flight characteristics and processing parameters. Moreover, some auxiliary post-treatments have been used in densification, such as silica sols[14], acidic phosphate solution sealing[15], zirconium and yttrium nitrate solution infiltration[6], sol immersion[16], spark plasma sintering[17], and laser glazing[18]. Compared with the electrolyte coating fabricated by APS in Fig.10, the electrolyte by SPS has better performances, including enough melting of sprayed particles, tight contact among the flats, and dense coating microstructure, as shown in Fig.9. All these mentioned above can effectively improve the conductivity and mechanical strength of the electrolyte coatings. The enhanced mechanical strength can alleviate spallation and delamination resulting from the mismatch of thermal

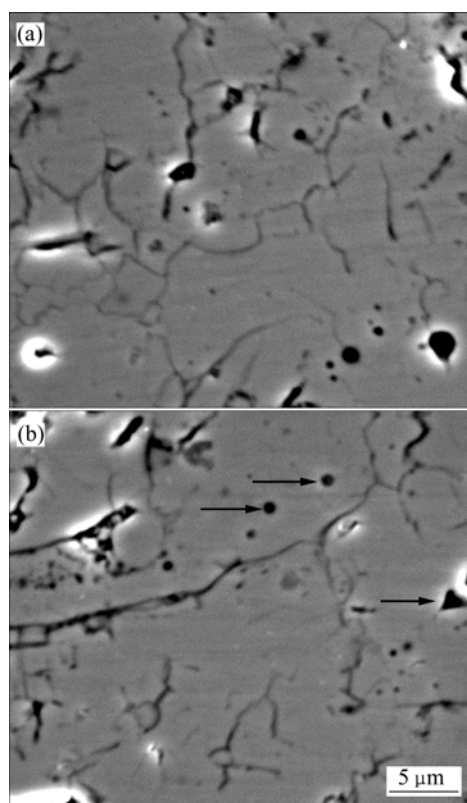


**Fig.10** SEM micrographs of cross-section for electrolyte fabricated by APS with voids (a) and cracks (b)

expansion coefficient.

The comparison of electrolytes of SOFC prepared by SPS and APS shows that higher densification, less thickness and more homogeneous component distribution of the electrolyte by SPS are observed. Therefore, the hybrid fabricating process, in which APS is selected for the porous cathode and anode and SPS for the dense and thin electrolyte, should be a better choice for the SOFC applications. During this process, the powder feeding approach just needs to be adjusted for the different corresponding spraying methods. Furthermore, the hybrid approach, shown in Fig.4(a), can also be easy in automation and integration without increasing the plasma-spraying equipments.

## 4 Conclusions

1) The FGM PEN of planar SOFC was successfully prepared by APS process. The obtained composition profiles can be qualitatively verified by their microstructure. The better electrochemical performance evaluated by impedance spectroscopy indicates significant improvements.

2) Compared with the electrolyte fabricated by APS, higher densification, less thickness and more homogeneous material composition distribution by SPS

are observed. This can effectively improve the conductivity of electrolyte.

3) The new hybrid process of SPS and APS should be a better approach to fabricate the core components of SOFC based on the robotic technology, and is our research focus in the future.

## References

- [1] YAMAMOTO O. Solid oxide fuel cells: Fundamental aspects and prospects [J]. *Electrochim Acta*, 2000, 45(15/16): 2423–2435.
- [2] SINGHAL S C. Advance in solid oxide fuel cell technology [J]. *Solid State Ionics*, 2000, 135(1/4): 305–313.
- [3] SINGHAL S C. Solid oxide fuel cells for stationary, mobile, and military applications [J]. *Solid State Ionics*, 2002, 152/153: 405–410.
- [4] VAEN R, HATHIRAMANI D, MERTENS J, HAANAPPEL V A C, VINKE I C. Manufacturing of high performance solid oxide fuel cells (SOFCs) with atmospheric plasma spraying (APS) [J]. *Surf Coat Tech*, 2007, 202(3): 499–508.
- [5] FAUCHAIS P. Understanding plasma spraying [J]. *J Phys D—Appl Phys*, 2004, 37(9): R86–R108.
- [6] NING X J, LI C X, LI C J, YANG G J. Modification of microstructure and electrical conductivity of plasma-sprayed YSZ deposit through post-densification process [J]. *Mater Sci Eng A*, 2006, 428(1/2): 98–105.
- [7] KWON O, KUMMAR S, PARK S, LEE C. Comparison of solid oxide fuel cell anode coatings prepared from different feedstock powders by atmospheric plasma spray method [J]. *J Power Sources*, 2007, 171(2): 441–447.
- [8] LIM D P, LIM D S, OH J S, LYU I W. Influence of post-treatments on the contact resistance of plasma-sprayed  $\text{La}_{0.8}\text{Sr}_{0.2}\text{MnO}_3$  coating on SOFC metallic interconnector [J]. *Surf Coat Tech*, 2005, 200(5/6): 1248–1251.
- [9] FAUCHAIS P, RAT V, DELBOS C, COUDERT J F, CHARTIER T, BIANCHI L. Understanding of suspension DC plasma spraying of finely structured coatings for SOFC [J]. *IEEE T Plasma Sci*, 2005, 33(2): 920–930.
- [10] FAUCHAIS P, ETCHART-SALAS R, DELBOS C, TOGNONVI M, RAT V, COUDERT J F, CHARTIER T. Suspension and solution plasma spraying of finely structured layers: Potential application to SOFCs [J]. *J Phys D—Appl Phys*, 2007, 40: 2394–2406.
- [11] FAUCHAIS P, ETCHART-SALAS R, RAT V, COUDERT J F, CARON N, WITTMANN-TÉNÈZE K. Parameters controlling liquid plasma spraying: Solutions, sols, or suspensions [J]. *J Therm Spray Tech*, 2008, 17(1): 31–59.
- [12] KASSNER H, SIEGERT R, HATHIRAMANI D, VASSEN R, STOEVEER D. Application of suspension plasma spraying (SPS) for manufacture of ceramic coatings [J]. *J Therm Spray Tech*, 2008, 17(1): 115–123.
- [13] LIU Shi-min, XING Chang-sheng, QIAN Xiao-liang. Synthesis of  $\text{La}_{0.8}\text{Sr}_{0.2}\text{Co}_{0.5}\text{Fe}_{0.5}\text{O}_3$  nanometer-size powders and its characterization [J]. *Journal of Huazhong University of Science and Technology: Natural Science*, 2005, 33(1): 81–83. (in Chinese)
- [14] MARPLE VOYER J, BÉCHARD P. Sol infiltration and heat treatment of alumina-chromia plasma-sprayed coatings [J]. *J Eur Ceram Soc*, 2001, 21(7): 861–868.
- [15] AHMANIEMI S, VUORISTO P, MÄNTYLÄ T. Improved sealing treatments for thick thermal barrier coatings [J]. *Surf Coat Tech*, 2002, 151/152: 412–417.
- [16] VIAZZI C, BONINO J P, ANSART F. Synthesis by sol-gel route and characterization of yttria stabilized zirconia coatings for thermal barrier applications [J]. *Surf Coat Tech*, 2006, 201(7): 3889–3893.
- [17] KHOR K A, YU L G, CHAN S H, CHEN X J. Densification of plasma sprayed YSZ electrolytes by spark plasma sintering [J]. *J Eur Ceram Soc*, 2003, 23(11): 1885–1863.
- [18] AHMANIEMI S, VIPPOLA M, VUORISTO P, MÄNTYLÄ T, CERNUSCHI F, LUTTEROTTI L. Modified thick thermal barrier coatings: Microstructural characterization [J]. *J Eur Ceram Soc*, 2004, 24(8): 2247–2258.

(Edited by YANG Bing)